

Article

# Triangular Cavity Multi-Passband HMSIW Filter Based on Odd-Even Mode Analysis

Luhua Zhang, Aiting Wu , Pengquan Zhang \* and Zhonghai Zhang

School of Electronics & Information, Hangzhou Dianzi University, Hangzhou 310018, China; 15738756303@163.com (L.Z.); zhanghaidong6388@163.com (Z.Z.)

\* Correspondence: wuaiting@hdu.edu.cn (A.W.); zpq@hdu.edu.cn (P.Z.)

**Abstract:** This letter proposes a multi-passband half-mode substrate integrated waveguide (HMSIW) filter based on the theory of odd and even mode analysis. The filter adopts a triangular HMSIW cavity cut along the diagonal of the rectangle. By etching two dual-mode resonators, the resonant mode of the HMSIW resonator is coupled with the odd-even mode of the dual-mode resonator to achieve multiple passbands. The defected ground structure (DGS) of the filter can reduce the resonance frequency of the HMSIW cavity without increasing the volume of the HMSIW cavity, making it easier to couple with the odd and even mode frequencies of the resonator. The input and output ports are directly coupled through a microstrip line. In this way, it adds an additional coupling path to the filter, which increases the out-of-band suppression without changing the performance in the passband, and improves the overall performance of the filter. To prove the feasibility of the above method, a multi-passband HMSIW filter was fabricated and tested. The center frequencies of the three passbands of the filter are 2.98 GHz, 4.78 GHz, and 6.62 GHz, respectively. The return loss in the passband is better than  $-15$  dB, and the insertion loss is better than 2 dB. The measured results have a good agreement with the simulation results.



**Citation:** Zhang, L.; Wu, A.; Zhang, P.; Zhang, Z. Triangular Cavity Multi-Passband HMSIW Filter Based on Odd-Even Mode Analysis. *Electronics* **2021**, *10*, 2927. <https://doi.org/10.3390/electronics10232927>

Academic Editor: Alejandro Melcón Alvarez

Received: 26 October 2021  
Accepted: 24 November 2021  
Published: 25 November 2021

**Publisher's Note:** MDPI stays neutral with regard to jurisdictional claims in published maps and institutional affiliations.



**Copyright:** © 2021 by the authors. Licensee MDPI, Basel, Switzerland. This article is an open access article distributed under the terms and conditions of the Creative Commons Attribution (CC BY) license (<https://creativecommons.org/licenses/by/4.0/>).

**Keywords:** HMSIW; dual-mode resonator; even-odd mode analysis; DGS; multiple passbands

## 1. Introduction

The development trend of modern wireless communication is multi-standard, multi-mode, ultra-wideband, and miniaturization. With the rapid development of communication systems, single-band communication systems can no longer meet people's daily needs. As a key device, multi-band filters have received more attention and research. Current research ideas for multi-passband filters: (1) use the different resonant frequencies of multi-mode resonators to achieve multi-passband response, and adjust the resonant frequencies of the fundamental mode and the higher-order mode by changing the electrical length and impedance [1]; (2) cascaded filter components [2,3]; (3) multi-passband response is achieved by connecting other frequency resonators in parallel in the resonant cavity. Since the substrate integrated waveguide (SIW) was proposed, the applications of SIW in antennas, couplers, and filters have emerged endlessly. Among them, half-mode substrate-integrated waveguide (HMSIW), quarter-mode substrate-integrated waveguide (QMSIW), eight-mode substrate-integrated waveguide (EMSIW), and even sixteenth-mode substrate-integrated waveguide (SMSIW) have been proposed and applied in succession [4,5]. Compared with the SIW structure, the QMSIW and EMSIW structures can make the filter more compact, but there are only TE modes in the QMSIW and EMSIW cavities, since TE<sub>102</sub> only has the equivalent magnetic wall along the longitudinal direction. The QMSIW, EMSIW structure resonator cavity cannot provide resonance environment for it. Therefore, in the low-order mode, only TE<sub>101</sub> mode and TE<sub>202</sub> exist in the two cavities [6]. The advantage of the HMSIW structure is that it reduces the volume of the filter by half, while still keeping the resonance mode of the full-mode SIW structure. DGS is one of the important technologies to realize circuit miniaturization, and this technology has attracted

wide attention in improving stopband performance and suppressing high-order harmonics. In addition, band-pass characteristics can be obtained by using the combination of the high-pass characteristics of the SIW structure and the low-pass characteristics of the DGS. DGS also has single-pole low-pass and cut-off frequency characteristics. Many studies have shown that combining these characteristics with the SIW structure can greatly improve the performance of the SIW filter [7].

In this paper, a multi-passband HMSIW filter using odd-even mode theory is proposed. Both DGS and slotline integration with HMSIW devices are leveraged in the proposed design. Compared with the existing filters, the proposed filter has a 3-passband with a more compact size. The dual-mode resonator is obtained by etching on the top metal layer of the cavity. The etched DGS is added to adjust the resonant frequency of TE<sub>102</sub> mode. The odd-even mode of the resonator is combined with the TE<sub>101</sub> and TE<sub>102</sub> resonant modes of the HMSIW to achieve three passbands. By changing of the electrical length of the dual-mode resonator, the odd and even mode frequency can be adjusted to achieve a tunable center frequency of the passband.

## 2. HMSIW Structure Analysis

The half-mode substrate integrated waveguide is obtained by cutting along a symmetry line of the full-mode substrate integrated waveguide structure. The symmetry plane of the SIW cavity is equivalent to an ideal magnetic wall, and the lines of electric field are parallel to the symmetry plane. Therefore, the HMSIW structure can reduce the volume by half, and ensure that the electric field structure in the SIW cavity is not affected. For a square cavity, there are two ways of cutting it symmetrically. One is cutting it horizontally or vertically. The other is cutting it diagonally [8]. Figure 1 shows the filter cut diagonally to form a resonant cavity in triangle.

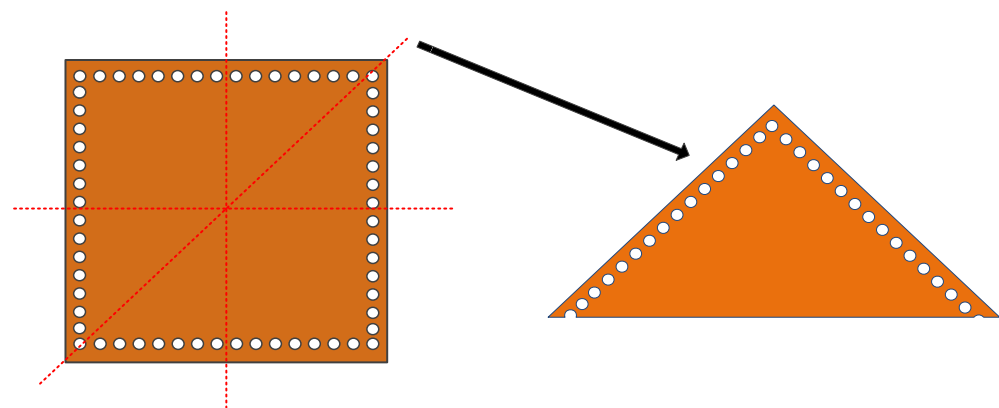


Figure 1. Diagonal cutting structure.

HFSS is used for the EM simulation, the analysis on the electric field of the HMSIW structure in the HFSS eigenmode, and the electric field distribution in the HMSIW cavity. Figure 2 shows the electric field distribution diagram of the diagonal cutting structure. It can be seen from the diagram that the HMSIW cavity does not destroy the electric field distribution. According to the electric field distribution, the resonant mode can be changed by perturbing the through hole, and the degenerate mode can be separated to realize the multi-passband response. If the dual-mode resonator is coupled with the HMSIW resonant mode, the odd-even mode of the dual-mode resonator and the TE<sub>101</sub> and TE<sub>102</sub> electric fields need to be coupled to each other to form a multiple passband. The size of the HMSIW resonant cavity determines the resonant frequency, and can be derived from the full-mode SIW resonant cavity resonant frequency formula [9]:

$$f_{TE_{m0n}} = \frac{c}{2\pi\sqrt{\mu_r\epsilon_r}} \sqrt{\left(\frac{m\pi}{W_{eff}}\right)^2 + \left(\frac{n\pi}{L_{eff}}\right)^2} \quad (1)$$

Among them,  $W_{eff} = W - \frac{d^2}{0.95p}$ ,  $L_{eff} = L - \frac{d^2}{0.95p}$ ,  $W_{eff}$ , and  $L_{eff}$  are the effective width and length of the SIW, respectively,  $d$  is the diameter of the metalized through hole, and  $p$  is the distance between the center of the metalized through hole. The odd-even mode frequency of the dual-mode resonator can be adjusted according to the electrical length of the odd-even model.

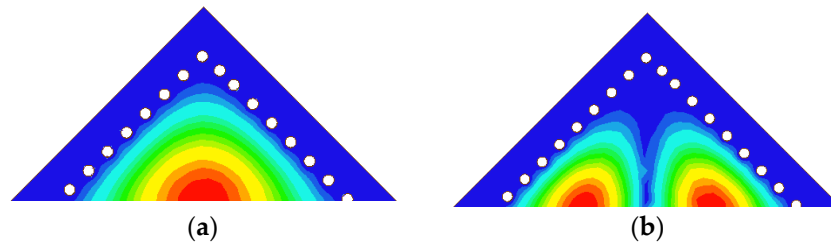


Figure 2. (a) TE101 electric field distribution diagram, (b) TE102 electric field distribution diagram.

### 3. Analysis of Dual-Mode Resonator

Figure 3 shows the geometry of the proposed dual-mode resonator. It can be that the resonator has good symmetry, and the frequency response conforms to the characteristics of the odd-even mode analysis. Therefore, it can be analyzed by the even-odd mode theory [10].

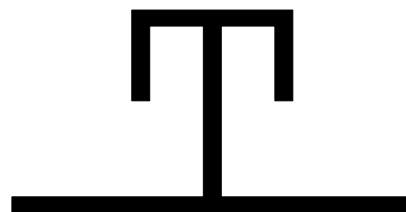


Figure 3. Geometry of the dual-mode resonator.

Generally, the slot line structure is based on the microstrip line theory, and the resonator is etched on the metal surface of the dielectric substrate. The etched slot type is equivalent to the slot line structure, which can be analyzed and calculated according to the transmission line impedance equation and the 1/4 transmission line theory. The dual-mode resonator adopts an E-type structure, and makes certain improvements to the structure, which is analyzed from the symmetry plane of the resonator. When analyzing odd modes, the symmetry plane of the resonator structure is equivalent to a short circuit. The symmetry plane of the even-mode resonator structure is equivalent to an open circuit. The equivalent circuit model is shown in Figure 4.

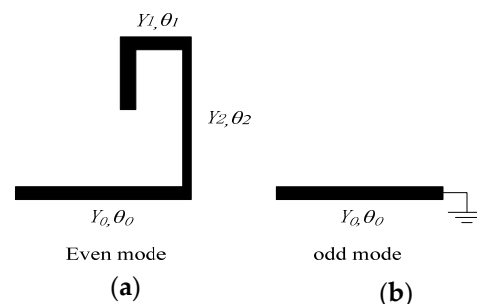


Figure 4. (a) Equivalent circuit of the even mode; (b) equivalent circuit of the odd mode.

In Figure 4,  $Y_0$ ,  $Y_1$ ,  $Y_2$ ,  $\theta_0$ ,  $\theta_1$ , and  $\theta_2$  represent the equivalent admittance and electrical length of the microstrip line in the equivalent circuit of the even-odd mode of the resonator,

respectively. Firstly, the odd-mode resonance frequency analysis is relatively simple, which is equivalent to a short-circuit transmission line, so its input admittance is [11]:

$$Y_{in,odd} = -jY_0 \cot\theta_0 \quad (2)$$

Let input admittance  $Y_{in,odd} = 0$ , according to the theory of quarter-wavelength transmission line resonator, we can obtain:

$$f_{odd} = \frac{c}{4l\sqrt{\epsilon_r}} \quad (3)$$

Similarly, analyze the resonant frequency of the even-mode, which is equivalent to a cascade of three transmission lines with different impedances and different electrical lengths, thus:

$$Y_{in,even} = -jY_0 \frac{Y_2 \tan\theta_2 + Y_1 \tan\theta_1 + Y_0 \tan\theta_0}{Y_0 - (\tan\theta_1 + Y_1 \tan\theta_1) \tan\theta_0} \quad (4)$$

Let input admittance  $Y_{in,even} = 0$ , thus:

$$Y_2 \tan\theta_2 + Y_1 \tan\theta_1 + Y_0 \tan\theta_0 = 0 \quad (5)$$

The even mode resonant frequency can be calculated according to the formula (5). The odd and even mode frequencies of the dual-mode resonator are coupled with the resonant frequencies of the TE<sub>101</sub> and TE<sub>102</sub> modes of the HMSIW cavity to form a multi-passband.

Therefore, it can be seen from the description of the above working principle that the analysis of the odd mode is simple. The formula (3) shows that controlling the electrical length  $\theta_0$  can control the odd-mode frequency. Equivalent circuit of the even mode is the cascade of multi-stage microstrip lines with different admittances, thus there are more degrees of freedom to control the resonant frequency of the even-mode.

## 4. Analysis and Design of Multi-Passband Filter

### 4.1. Filter Structure

Through the above analysis of the HMSIW resonator cavity and the theoretical analysis of the dual-mode resonator, it can be demonstrated that the natural resonant mode of the HMSIW resonator is coupled with the odd-even mode of the dual-mode resonator to form a multiple passband. In addition to etching the dual-mode resonator on the front metal surface of the filter, DGS [12] is also etched on the ground layer on the reverse side. In addition, it also provides an additional electrical coupling between the input and output ports, which improves the filter's out-of-band suppression. Figure 5 shows the structure and coupling topology of the filter designed in this letter, and the dimensions are shown in Table 1. From the topology diagram in Figure 5c, it can be seen that the low frequency band is TE<sub>101</sub> mode, the middle passband is the coupling of the even mode frequency of the resonator and the TE<sub>102</sub> mode, and the high frequency end passband is the odd mode frequency of the resonator.

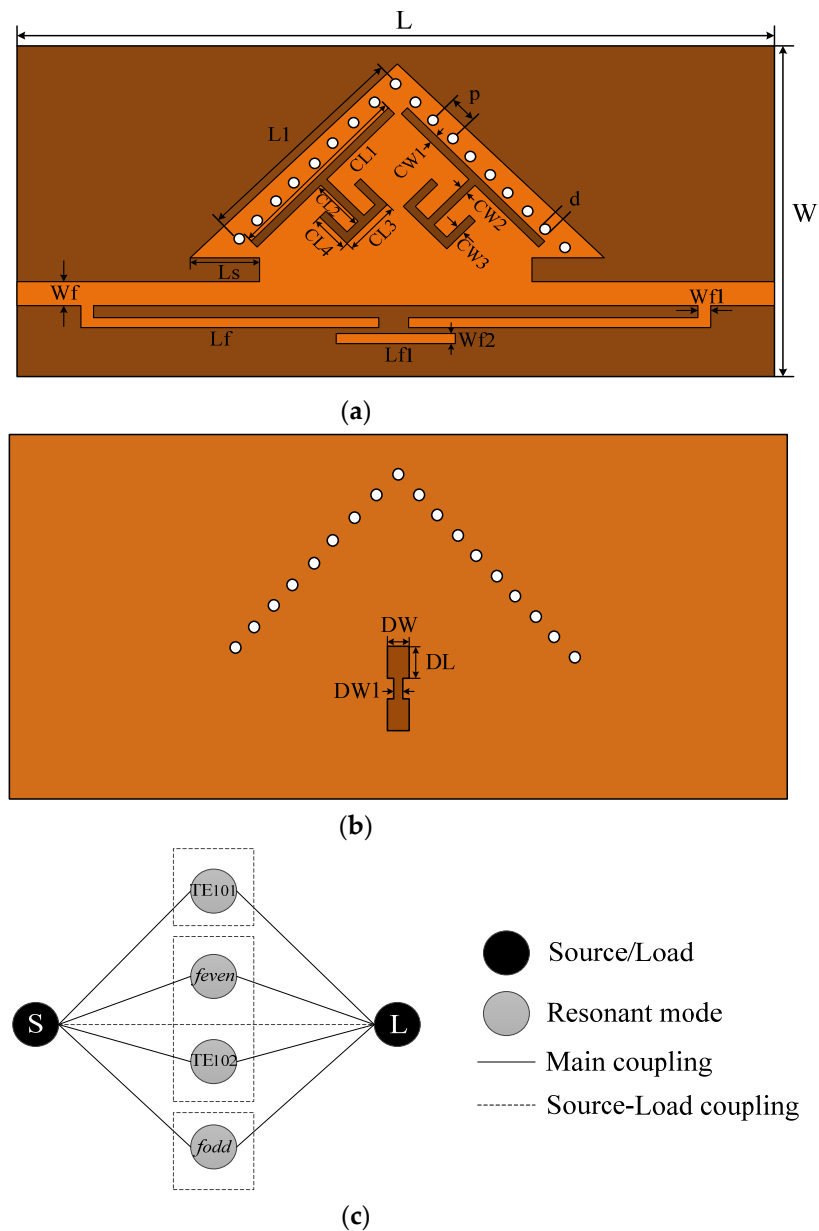


**Figure 5.** (a) Filter front structure diagram; (b) filter reverse structure diagram; (c) coupling topology diagram.

**Table 1.** Filter size table.

Parameter	W	L	Wf	L1	CL1	CL2	Lf
Value (mm)	20	40	0.9	13.2	10.8	3.4	16.95
Parameter	CL3	CL4	CW1	CW2	CW3	Ls	Lf1
Value (mm)	3	2.6	0.6	0.6	0.5	4.1	7
Parameter	Wf1	d	p	h	DW	DW1	DL
Value (mm)	0.65	0.5	1.2	0.635	1.4	0.6	1.6

#### 4.2. Filter Design Analysis

The HFSS simulation shows that etching DGS can reduce the resonant frequency of the HMSIW resonant cavity TE102. As shown in Figure 6, with the etched DGS, the resonant frequency of TE102 mode is significantly reduced from 7.9 GHz to 7.42 GHz, which makes

the TE<sub>102</sub> mode more easily coupled with the even mode of the resonator. It also facilitates the filter miniaturization. In addition, the direct coupling between the input and output ports is introduced through the microstrip line, and a transmission zero (TZ) of the low frequency band of the TE<sub>101</sub> mode is generated at 3.74 GHz. Therefore, the out-of-band suppression performance of the filter is significantly improved.

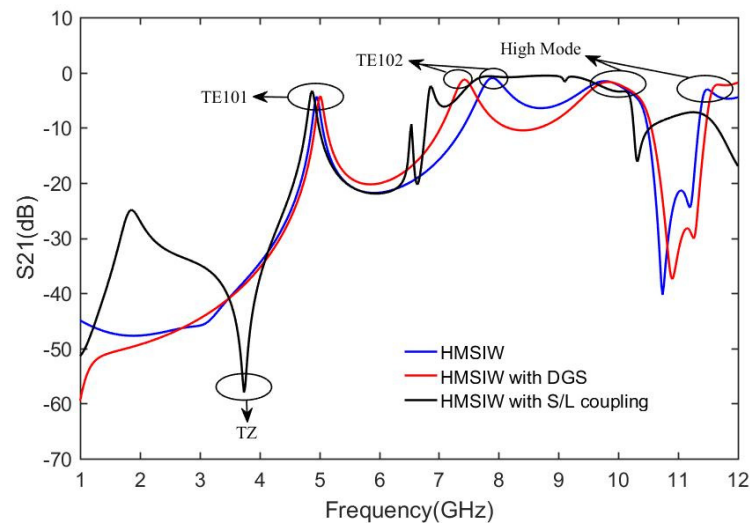


**Figure 6.** HMSIW resonant cavity adding DGS structure and source-load direct coupling analysis diagram.

After adding the dual-mode resonator, the filter is simulated, and the simulation result is shown in Figure 7. It can be seen that the formation of the three passbands is consistent with the above analysis. When the DGS is not etched, it is difficult for the TE<sub>102</sub> mode to couple with the even-mode mode of the resonator to form a passband. Therefore, etching DGS can shift TE<sub>102</sub> mode resonant frequency to low frequency without increasing HMSIW resonant cavity volume. This achieves miniaturization to a certain extent.

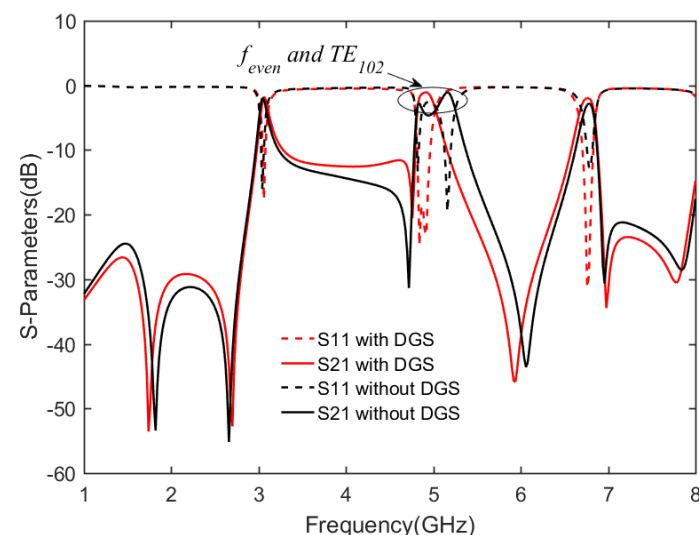
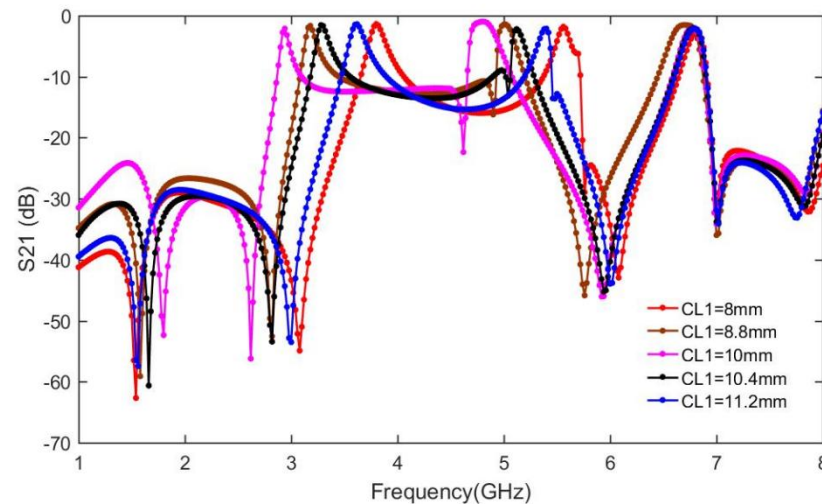


**Figure 7.** S-parameter comparison analysis diagram after adding dual-mode resonator.

#### 4.3. Resonator Parameters Analysis

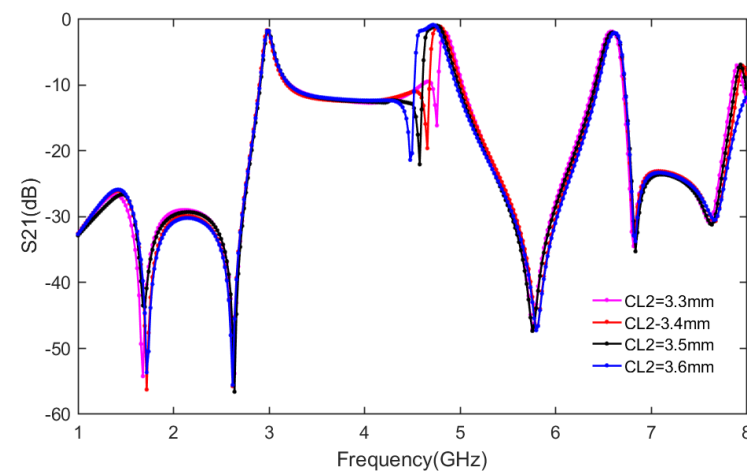
In Figure 8, combining the odd-even model and the filter structure diagram, it can be found that changing the length of the CL1 slot line can control the center frequency of the odd-even mode. The CL1 slot line is a common part in the equivalent circuit of the even-odd mode, so changing the length of the CL1 slot line can control the resonant

frequency of the odd-even mode at the same time. Since the CL1 slot line is etched at the edge of the resonant cavity, the magnetic field is the strongest and the electric field is the weakest. Therefore, the change of the CL1 slot line will destroy the field strength of the TE<sub>101</sub> mode, and subsequently affect the center frequency of the first passband. The center frequencies of three passbands will be affected when changing CL1



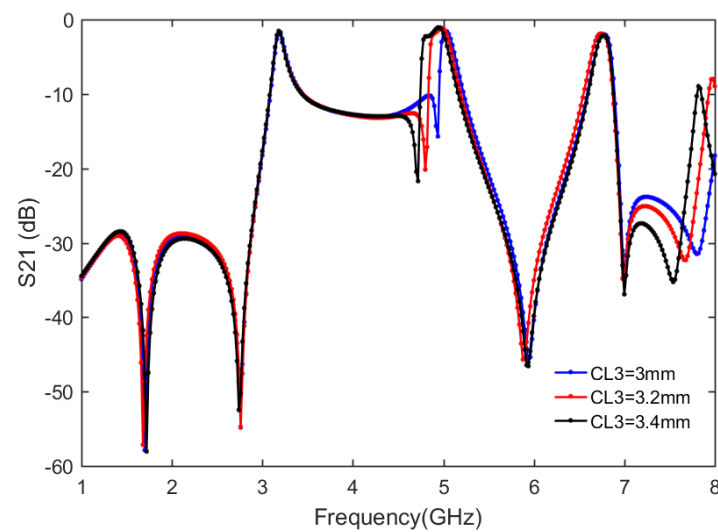
**Figure 8.** Variation curve of S21 with CL1.

Figure 9 shows that CL2 length has a direct impact on the center frequency of the second passband, but little impacts on the first and the third passbands. The reason is that CL2 mainly affects the even mode of the dual mode resonator. In addition, the even mode contributes to the second passband most.



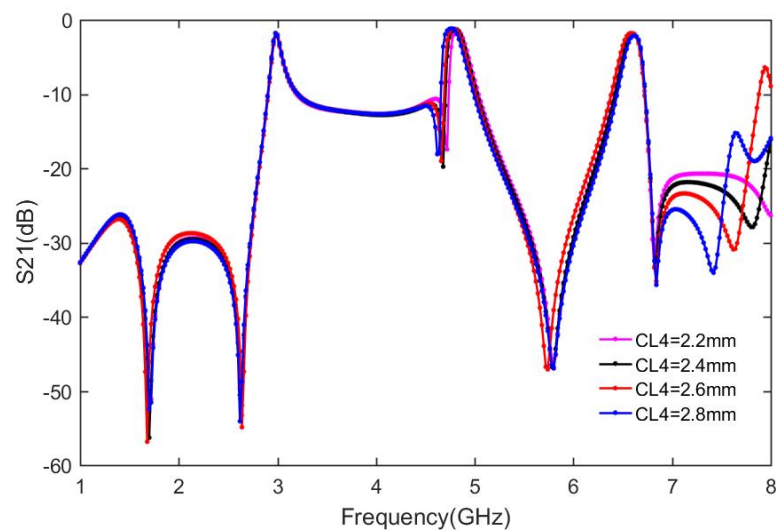
**Figure 9.** Variation curve of S21 with CL2.

Figure 10 indicates that CL3 could also affect the center frequency of the second passband. The reason is similar to CL2's impact. In addition, CL2 and CL3 could adjust the center frequency of the second passband independently.



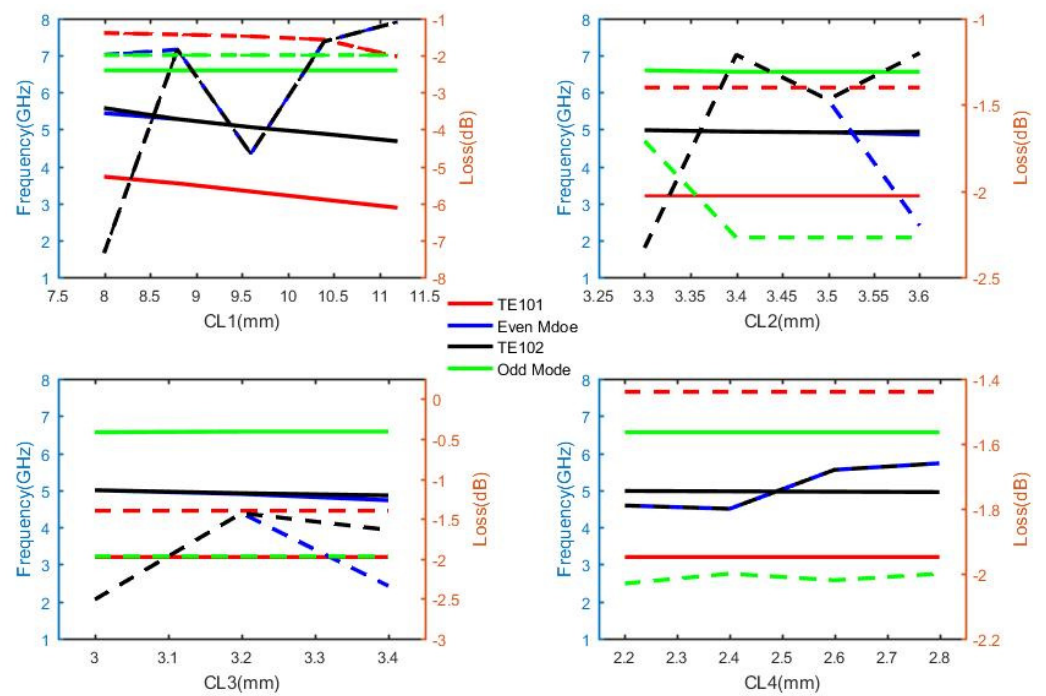
**Figure 10.** Variation curve of S21 with CL3.

In Figure 11, changing the length of CL4 slot line can control the resonant frequency of the even mode, that is, the center frequency of the second passband. It can be seen from Figure 4b that the odd-mode model does not include the CL4 slot line. Changing the length of the CL4 slot line can independently control the resonance frequency of the even mode. Therefore, CL4 slot line controls the center frequency of the second passband, and the center frequency of the first passband and the third passband are basically unchanged. Compared with CL4 slot line, the change of CL3 slot line has a greater impact on the electric field, thus the change of even mode frequency is more sensitive when the length of CL3 slot line is changed.



**Figure 11.** Variation curve of S21 with CL4.

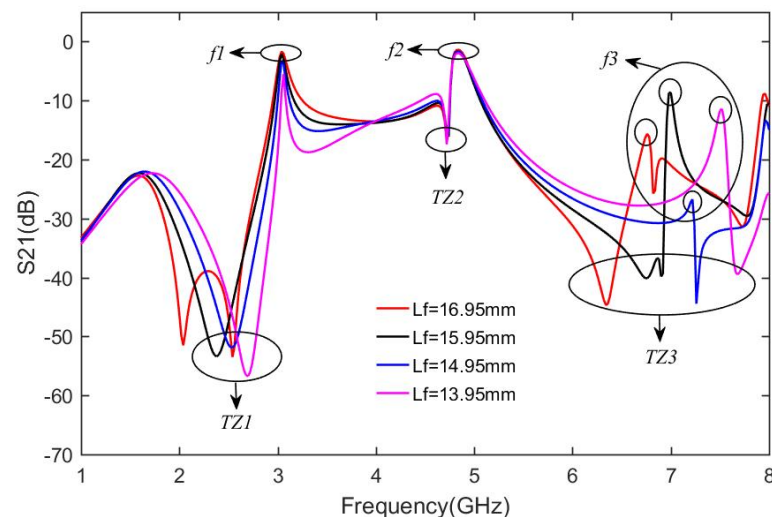
The influences of CL1-CL4 on the frequency and loss of different modes are analyzed. Figure 12 shows that CL1 has an impact on the frequencies of the four resonant modes, mainly for TE<sub>101</sub>, TE<sub>102</sub>, and even mode modes. According to the loss curve, CL1 has a considerable impact on the loss of the second passband. The influences of CL2 and CL3 are mainly on the second passband, and little on the first and third passband response, shown by the TE<sub>102</sub> and even-mode loss curves. CL4 has a slight influence on the second passband, and little impact on the other two.



**Figure 12.** The influence of CL1-CL4 on frequency and loss of different modes (the solid lines correspond to the left vertical axis, the frequency. The dotted lines correspond to the right vertical axis, the loss.)

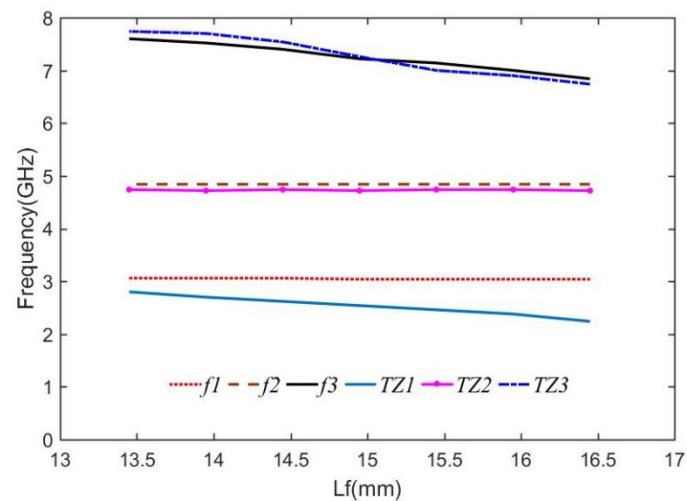
#### 4.4. Source and Load Coupling Analysis

It can be seen from Figure 5a that the coupling between the source and the load is contributed by  $L_f$  and  $L_{f1}$ . As shown in Figure 13,  $f_1$ ,  $f_2$ , and  $f_3$  are the resonance frequencies of the three passbands, respectively. TZ1, TZ2, and TZ3 are the transmission zeros near the passbands. Without  $L_{f1}$ , TZ1 can be adjusted by changing the value of  $L_f$ . However, the fluctuation of the third passband is very unstable as  $L_f$  changes.



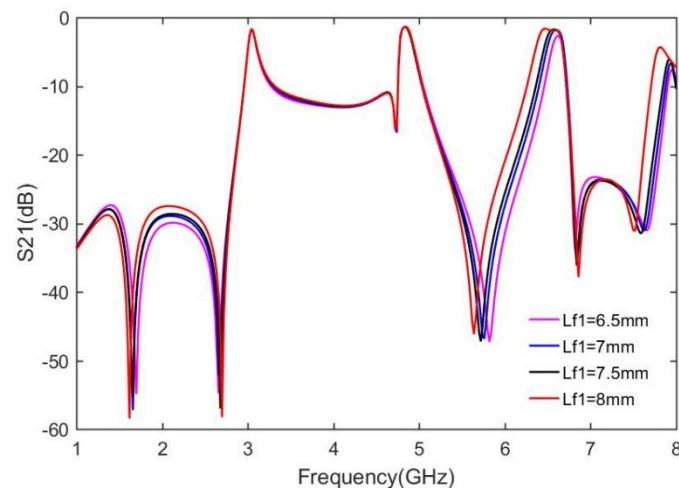
**Figure 13.** Variation curve of S21 with  $L_f$ .

Figure 14 shows the influence of the parameter  $L_f$  on the three resonant frequencies and TZ of the filter. As  $L_f$  increases, the coupling between the source and the load increases, TZ1 and TZ3 shift to lower frequencies, and TZ2 remains the same.  $f_1$  and  $f_2$  are basically not affected by  $L_f$ .  $f_3$  decreases as  $L_f$  increases. With Figure 14, it is convenient to adjust the first and the third passband.



**Figure 14.** Change graph of the three resonance frequencies and transmission zero point of  $L_f$ .

$L_{f1}$  is added to improve both the first and the third passband. Comparing Figure 15 with Figure 14, it could be seen that the loss becomes much more stable, indicating the impedance matching is improved for the third passband. Moreover, the out-of-band suppression at the low frequency of the first passband is also improved.



**Figure 15.** Variation curve of  $S_{21}$  with  $L_{f1}$ .

#### 4.5. Simulation Result Analysis

Simulation of the proposed filter is carried out using the full-wave EM simulator HFSS (solution type = driven model, frequency range = 1–8 GHz, step size = 0.02 GHz, type of sweep = fast, maximum number of passes = 16, maximum delta energy = 0.05, type of ports = wave-ports, and boundary condition = radiating only in all direction). Through HFSS simulation, it is obtained that the center frequency of the first passband of the filter is 2.98 GHz, the return loss  $S_{11}$  in the passband is better than  $-15$  dB, the insertion loss  $S_{21}$  is  $-1.7$  dB and the 3 dB bandwidth is 40 MHz. The center frequency of the second passband is 4.78 GHz, the return loss  $S_{11}$  in the passband is better than  $-20$  dB, the insertion loss  $S_{21}$  is  $-1.1$  dB and the 3 dB bandwidth is 170 MHz. The center frequency of the third passband is 6.62 GHz, the return loss  $S_{11}$  in the passband is better than  $-20$  dB, the insertion loss  $S_{21}$  is  $-2$  dB and the 3 dB bandwidth is 110 MHz. Figure 16 shows that the proposed filter has six transmission zeros ( $TZ_1$ – $TZ_6$ ), which are located at 1.7 GHz, 2.62 GHz, 4.64 GHz, 5.78 GHz, 6.82 GHz, and 7.64 GHz, respectively. These transmission zeros increase the overall out-of-band rejection of the filter.

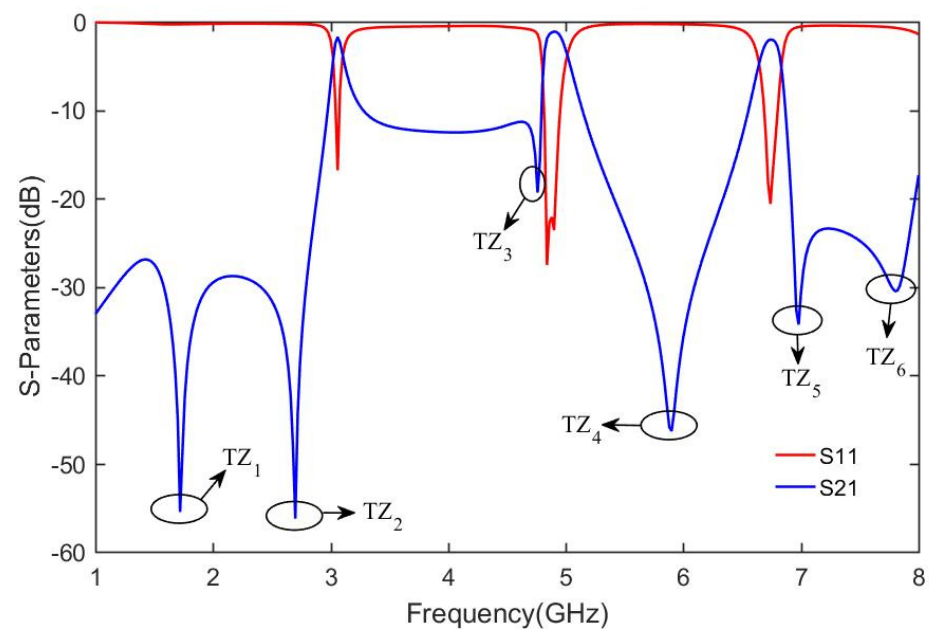


**Figure 16.** Simulated S-parameters of the filter.

From the analysis in the above section, we can see that changing the CL1 parameter can affect the center frequency of the first passband, and the bandwidth will also change, the maximum that it can be changed to being 110 MHz. There are many parameters that affect the response of the second passband, but the CL2 and CL3 parameters have the greatest impact. It is difficult to change the resonator parameters to make the third passband change significantly. Only when the Lf1 parameter is changed do the center frequency and bandwidth of the third passband change significantly. The specific bandwidth information is shown in Table 2.

**Table 2.** The influence of CL1, CL2, CL3, and Lf1 on the bandwidths of the three passbands.

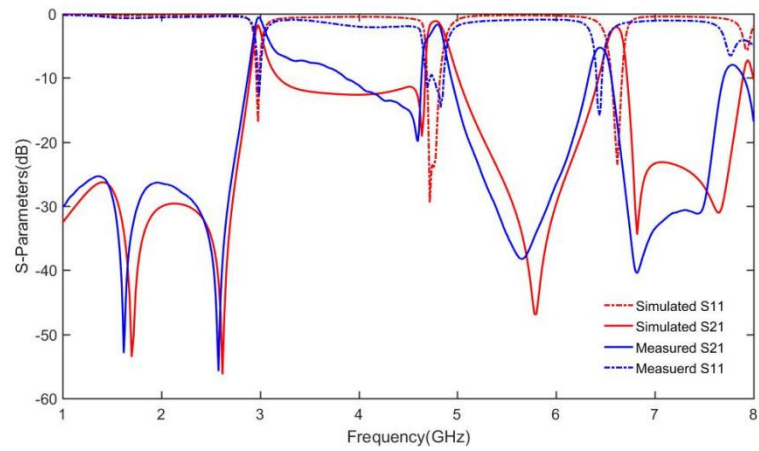
	3 dB BANDWIDTH of Simulate	Influence Bandwidth Parameters	Bandwidth Adjustable Range
The first passband	40 MHz	CL1	40~110 MHz
The second passband	170 MHz	CL2 or CL3	50~250 MHz
The third passband	110 MHz	Lf1	110~370 MHz

The influences of the related parameters on the bandwidths of the 3 resonances are summarized in Table 2. The first passband bandwidth is mainly affected by CL1, and its maximum bandwidth could reach to 110 MHz. CL2 and CL3 have the most contribution to the second passband bandwidth. The center frequency and bandwidth of the third passband is mainly controlled by Lf1.

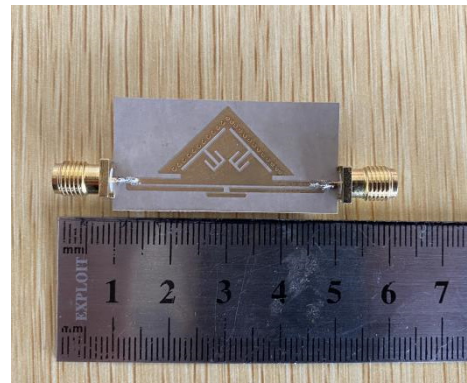
## 5. Results and Discussion

The filter uses Rogers RT6006 dielectric substrate with a thickness of 0.653 mm, a dielectric constant of 6.15, and a loss angle of 0.0019. The material of the upper and lower metal layers of the dielectric substrate is copper, and the thickness of the copper is 0.035 mm. In order to verify the performance of the filter, the filter was fabricated and measured, as shown in Figure 17. The tests were performed using a Rohde & Schwarz ZVA24. Before the test, the instrument was calibrated, and then IFBW was set to 1 KHz, 901 of points, and the input power was 0 dBm. It can be seen that the simulation results are basically consistent with the measured results. This filter can be used in the Sub-6 GHz frequency band in the 5G communication band. The feasibility of the method is verified by

the experiments. Comparisons between the proposed filter and other filters in performance are as shown in Table 3.



(a)



(b)



(c)

Figure 17. (a) Comparison of simulation and measurement (b) front view of filter (c) rear view of filter.

Table 3. Comparison with other filters in performance.

Reference	$f_0$ (GHz)	IL (dB)	Size ( $\lambda_g \times \lambda_g$ )	No. of TZs	Cavity Shape	No. of Layers
6	8.22/11.97	-1.18/-1.09	$0.96 \times 0.43$	3	rectangle	1
7	8.15/10.15/12.85	-1.05/-1.1/-1.2	$0.4 \times 0.4$	5	fan	2
8	5.37/10.38	-1.35/-1.38	$0.4 \times 0.4$	2	rectangle	1
10	3.6/6.4	-1.3/-1.2	$0.29 \times 0.29$	3	rectangle	1
This work	2.98/4.78/6.62	-1.1/-1.6/-4.92	$0.4 \times 0.2$	6	triangle	1

$\lambda_g$ : the guided wavelength of the first passband.

## 6. Conclusions

In this letter, a HMSIW filter based on odd-even mode analysis is designed to achieve multi-pass band by etching a dual-mode resonator on HMSIW. Two dual-mode resonators improve the odd-even mode resonant frequency, coupled with the inherent resonant frequency of HMSIW resonant cavity. Changing the length of the slot line of the odd-even model can flexibly adjust the center frequency of the passband. Etching the DGS can reduce the resonant frequency without increasing the volume of the resonant cavity and reduce the volume of the filter. Finally, the input-output direct coupling structure optimizes the out-of-band rejection while maintaining the passband performance, and improves the

filter performance. The filter has a small size, the overall size is only  $0.4 \lambda_g \times 0.2 \lambda_g$ , and it can be applied in the 5G band Sub-6 GHz frequency band communication, such as n79 band. This multi-band application structure is more suitable for the development of integrated circuits.

**Author Contributions:** Writing—original draft preparation, L.Z.; Supervision and modification, A.W., P.Z. and Z.Z. All authors have read and agreed to the published version of the manuscript.

**Funding:** This work was funded by the Education Department of Zhejiang Province, China (No. Y202044273) and National Natural Science foundation of China (Grant 61501153).

**Institutional Review Board Statement:** Not applicable.

**Informed Consent Statement:** Not applicable.

**Data Availability Statement:** Data sharing not applicable.

**Conflicts of Interest:** The authors declare no conflict of interest.

## References

1. Zhao, Y.; Zhou, C.; Guo, X.; Wu, W. Design of Four-pass Band Filter Based on Substrate Integrated Waveguide. *J. Microw.* **2017**, *33*, 152–156.
2. Abu-Hudrouss, A.M.; Lancaster, M.J. Design of multiple-band microwave filters using cascaded filter elements. *J. Electromagn. Waves Appl.* **2009**, *23*, 2109–2118. [[CrossRef](#)]
3. Tsai, L.-C.; Hsue, C.-W. Dual-band bandpass filters using equallength coupled-serial-shunted lines and Z-transform technique. *IEEE Trans. Microw. Theory Tech.* **2004**, *52*, 1111–1117. [[CrossRef](#)]
4. Shen, W. Extended-doublet half-mode substrate integrated waveguide bandpass filter with wide stopband. *IEEE Microw. Wirel. Compon. Lett.* **2018**, *28*, 305–307. [[CrossRef](#)]
5. Wang, S.; Zhang, D.; Zhang, Y.; Qing, L.; Zhou, D. Novel dual-mode bandpass filters based on SIW resonators under different boundaries. *IEEE Microw. Wirel. Compon. Lett.* **2017**, *27*, 28–30. [[CrossRef](#)]
6. Zhang, G.; Huang, Y. Design of compact filter Based on EMSIW structure and QMSIW Structure. *Electron. Devices* **2019**, *42*, 1174–1178.
7. Grine, F.; Ammari, H.; Benhabiles, M.T.; Riabi, M.L. Double-layer Sixteenth-mode Substrate Integrated Waveguide Filter based on Defected Ground Structure. In Proceedings of the 2019 IEEE MTT-S International Microwave Workshop Series on Advanced Materials and Processes for RF and THz Applications (IMWS-AMP), Bochum, Germany, 16–18 July 2019; pp. 55–57.
8. Guo, Y. *Research on Multi-Frequency Miniaturized Filter Based on Substrate Integrated Waveguide*; China University of Mining and Technology: Xuzhou, China, 2020.
9. Pelluri, S.; Fasil, M.; Mondal, D.; Kartikeyan, M.V. Dual-band Bandpass filter using SIW cavity with E-shaped DGS. In Proceedings of the 2020 URSI Regional Conference on Radio Science (URSI-RCRS), Varanasi, India, 12–14 February 2020; pp. 1–3.
10. Zhang, D.; Wang, S.; Liu, Q.; Zhou, D.; Zhang, Y.; Lv, D.; Wu, Y. Design of dual-pass band-pass filter with four-mode resonator structure based on odd-even mode analysis method. *Chin. J. Electron.* **2018**, *46*, 387–392.
11. Zhang, H.; Kang, W.; Wu, W. Miniaturized Dual-Band SIW Filters Using E-Shaped Slotlines with Controllable Center Frequencies. *IEEE Microw. Wirel. Compon. Lett.* **2018**, *28*, 311–313. [[CrossRef](#)]
12. Zhao, X.; Liu, J. Analysis and Design of SIW-DGS Wideband Bandpass Filter. *J. Microw.* **2012**, *28*, 182–186.